


RESEARCH ARTICLE

Comparison of the Impacts of Three Types of Plasma-Activated Water on the Seed Germination and Plant Growth of Lettuce (*Lactuca sativa*)

Ramin Mehrabifard  | Adriana Mišúthová | Zdenko Machala 

Division of Environmental Physics, Faculty of Mathematics, Physics and Informatics, Comenius University, Bratislava, Slovakia

Correspondence: Zdenko Machala (machala@fmph.uniba.sk)

Received: 1 May 2025 | **Revised:** 23 September 2025 | **Accepted:** 26 September 2025

Funding: This study was funded by EU NextGenerationEU through the Recovery and Resilience Plan for Slovakia under the Project No. 09I03-03-V03-00033 EnvAdvice and the Slovak Research and Development Agency APVV-22-0247.

Keywords: dielectric barrier discharge | lettuce seed and plant | plasma-activated water | RONS | seed germination | transient spark, microwave plasma

ABSTRACT

Cold air plasma typically generates reactive oxygen and nitrogen species (RONS), which are transported into water to produce plasma-activated water (PAW). This study examines the effect of PAW produced by three different plasma systems on lettuce: transient spark, fountain dielectric barrier discharge, and microwave plasma. Physiochemical PAW properties and concentrations of RONS (ozone, hydrogen peroxide, nitrite, and nitrate) were measured. Seed germination parameters were recorded in 8-day paper tests. The effect of PAW irrigation was investigated after 6 weeks of plant growth in the soil by measuring the germination rate, plant and root length, dry and fresh plant weight, number of leaves, and photosynthetic pigments. PAW, dependent upon its RONS contents, enhances plant development and affects its physiological parameters.

1 | Introduction

In many parts of the world, agricultural cultivation is a significant economic sector. Fresh, high-quality agricultural goods with an appropriate amount of macro- and micronutrients are in high demand because they provide a decent quality of life. Many inorganic and organic fertilizers, which supply plant nutrients required for their development, are used to promote the growth of crops, fruits, and vegetables [1]. In addition to fertilizers, several physical techniques have also been used to promote the agricultural plant growth, such as pulsed electric fields or static magnetic fields [2, 3]. Cold (nonthermal, nonequilibrium) plasma (CP) also represents an innovative physical approach for plant growth promotion.

CP formed by different types of atmospheric pressure air discharges generates a very reactive atmosphere consisting of energetic electrons, radicals, and numerous gaseous reactive species such as $\bullet\text{OH}$, H_2O_2 , NO_x , and HNO_x [4, 5]. Upon

interaction with water, these species dissolve into the water and generate plasma-activated water (PAW). Long-lived reactive oxygen and nitrogen species (RONS) like H_2O_2 , NO_2^- , or NO_3^- are the most typical constituents of PAW, which can be regarded as a sustainable and clean substitute for chemical fertilizers. CP and PAW have a possibility to be efficiently employed in numerous agricultural uses [6–8].

Most of the current research of plasma agriculture application focuses on seed disinfection and enhanced germination, as well as promotion of the plant development, and other applications involving direct plasma treatment [9–13]. There is a growing interest in indirect plasma treatments on plants and seedlings, especially by the application of PAW, or plasma-activated fertilizer [14–19].

H_2O_2 , NO_2^- , and NO_3^- are the long-lived plasma-generated RONS typically present in the PAW. They may be readily

incorporated into plant cells where they can function as signaling molecules in plant physiology, or as sources of essential nitrogen nutrients for the plant. H_2O_2 may pass through a cell membrane either by free diffusion or through membrane proteins called aquaporins that help move water through the membrane [20]. H_2O_2 may be scavenged in the cell by the enzyme catalase, which produces oxygen and water, or by the antioxidant enzyme peroxidase. Since hydrogen peroxide (H_2O_2) is the most persistent reactive oxygen species (ROS), it is essential for intracellular communication in a variety of physiological functions.

One important source of nitrogen, a macronutrient that is vital to plants, is nitrate (NO_3^-). It is transported into plant cells by specific membrane transport proteins or concentration-dependent diffusion, which is a slower process [21, 22]. Furthermore, NO_3^- also functions as a signaling molecule, triggering the activation of genes necessary for absorption and self-transport inside the plant cell. Particularly for active photosynthesis and absorption in support of the biomass formation, the absorbed nitrogen might be used effectively. Certain plants can also use NO_2^- (nitrite) as a source of nitrogen; however, it may also be hazardous to many plants [23].

According to Gierczik et al. [24], the presence of H_2O_2 and NO_3^- in PAW improved seedling resistance to simultaneous low-temperature and hypoxic stress conditions during germination. Zhang et al. [25] demonstrated that they achieved 80% germination rates rather than 30% by employing plasma-activated tap water. Additionally, when compared to industrial synthetic fertilizer, plasma-activated tap water produced better rates of stem elongation and ultimate stem lengths. They concluded that these gains were mostly dependent on the mixture of two particular long-lived PAW species. Fan et al. [26] used deionized water exposed to CP to examine the impact of PAW on mung bean sprouts. By assessing factors including germination rate, growth characteristics, total phenolic and flavonoid levels, and antioxidant enzyme activity, they assessed the PAW impact and concluded that it might promote mung seed germination and growth.

In this study, we use three different plasma sources to generate RONS in water with different concentrations to investigate the effect of each species (NO_3^- , NO_2^- , H_2O_2) on lettuce seed and plant parameters separately. Prior to using PAW for the irrigation of target plant seedlings, concentrations of long-lived species (O_3 , H_2O_2 , NO_2^- , NO_3^-) were analyzed by UV-VIS absorption spectroscopy, along with the physiochemical parameters of PAW, such as pH, oxidation-reduction potential (ORP), total dissolved solids (TDS), electrical conductivity (EC), and temperature. Although all three types of PAW contain a mixture of RONS, water activated by MW plasma generates high concentrations of NO_3^- , transient spark (TS) generates the highest NO_2^- , and fountain dielectric barrier discharge (FDBD) provides lower RONS concentration than TS. O_3 concentration for all these PAW types is small. We examined specific germination and plant growth characteristics (germination, plant and root length, number of leaves, as well as fresh and dry weight) and physiological data, including the concentration of photosynthetic pigments, to assess the efficacy of PAW in enhancing germination and plant growth.

2 | Materials and Methods

2.1 | Plasma Setups

Experimental setups are shown in Figures 1–3. Three different discharge reactors are used for this experiment: Multipin TS discharge, FDBD, and microwave (MW) plasma. A high-voltage probe (Tektronix P6015A) is used for measuring voltage. A Rogowski current meter (Pearson Electronics 2877) measures the discharge current. Digitizing oscilloscope Tektronix TDS 2024 records and processes the time-dependent waveform of the electrical characteristics of the discharge (voltage and current). The same batch of tap water with a typical initial conductivity of $\sim 500 \mu\text{S}/\text{cm}$ was used to make all three types of PAW treatments, which also served as the untreated control (TW). This makes sure that plasma activation is the only process that changes the properties of the water. In contrast to deionized or distilled water, it is more abundant, more physiologically suitable for plants, and has a natural buffering capacity to maintain a stable pH due to its bicarbonate buffer system. PAWs were used for irrigation within 10 min of plasma activation to preserve their reactive species content.

2.1.1 | Multipin Transient Spark (TS)

Single TS discharge has been extensively investigated in our research group, including the setups with liquid electrode [27–29]. Here, we employ a Multipin TS that operates in pin-to-plane geometry with a common liquid grounded electrode. The power needle electrodes are connected to a DC power supply each separately through a $4.7 \text{ M}\Omega$ ballast resistor and 50 pF external capacitor. The discharge gap, from the tip of needle electrodes to the water surface is $\sim 1 \text{ cm}$ long. The plasma activation duration for water was established at 1 mL min^{-1} per electrode, meaning each mL of water was subjected to plasma activation for 1 min, which was kept constant throughout all tests. The batch volume of 210 mL of water was treated by TS plasma for 10 min by 21 electrodes. Figure 1A,B shows a schematic diagram and a real picture of the Multipin TS plasma source, and Figure 1C,D shows voltage and current–voltage waveform of the discharge, respectively.

The TS plasma power was measured using voltage, current, and frequency. The instantaneous power, $P(t)$, at any time t is given by:

$$P(t) = V(t) \cdot I(t)$$

where $V(t)$ is the instantaneous voltage and $I(t)$ is the instantaneous current. To find the average power over one period, we integrate $P(t)$ over the period (T) and divide by T , that is, multiply by the frequency (f):

$$P_{\text{avg}} = \frac{1}{T} \int_0^T P(t) dt = f \int_0^T V(t) \cdot I(t) dt.$$

The typical average power of the Multipin TS is 52.5 W , that is, 2.5 W/needle .

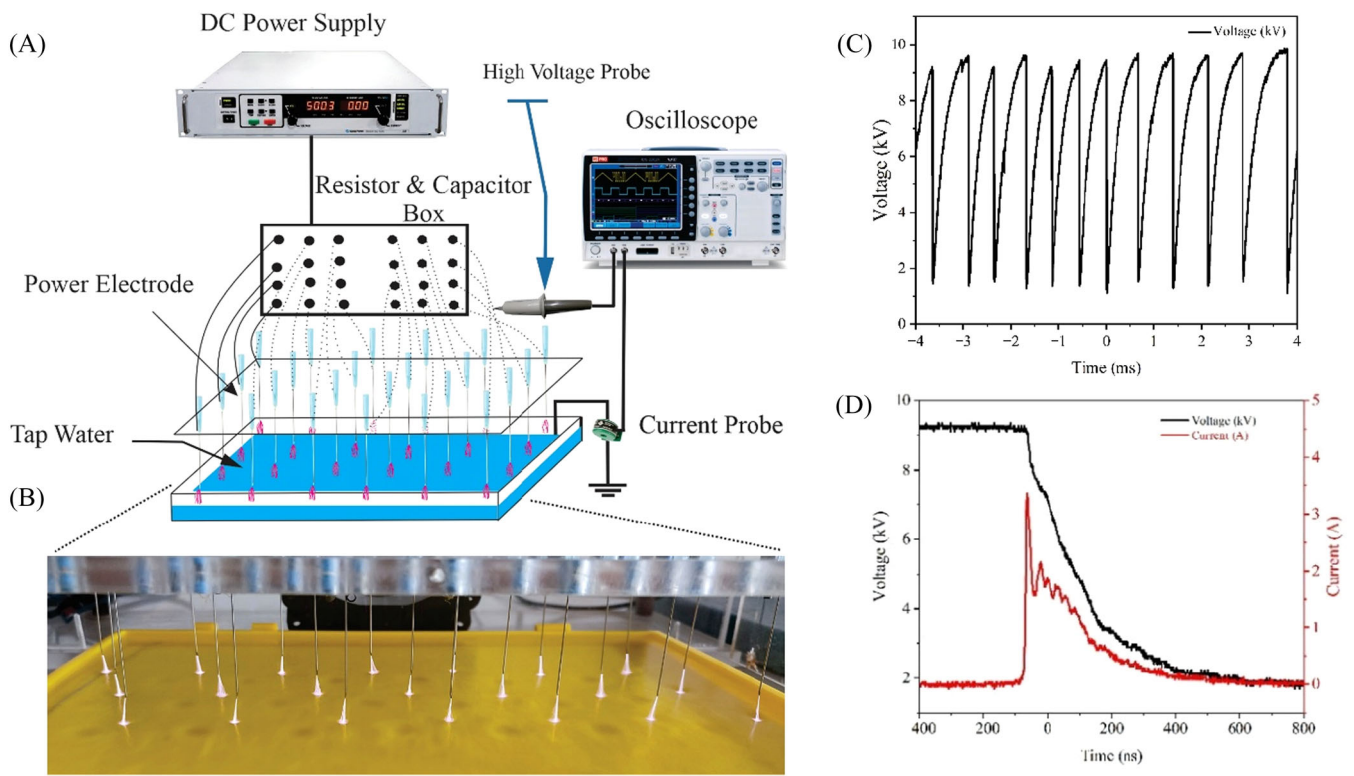


FIGURE 1 | Multipin TS discharge, (A) schematic diagram, (B) real photograph, (C) voltage waveform on ms timescale, and (D) current–voltage waveform on 100 ns timescale.

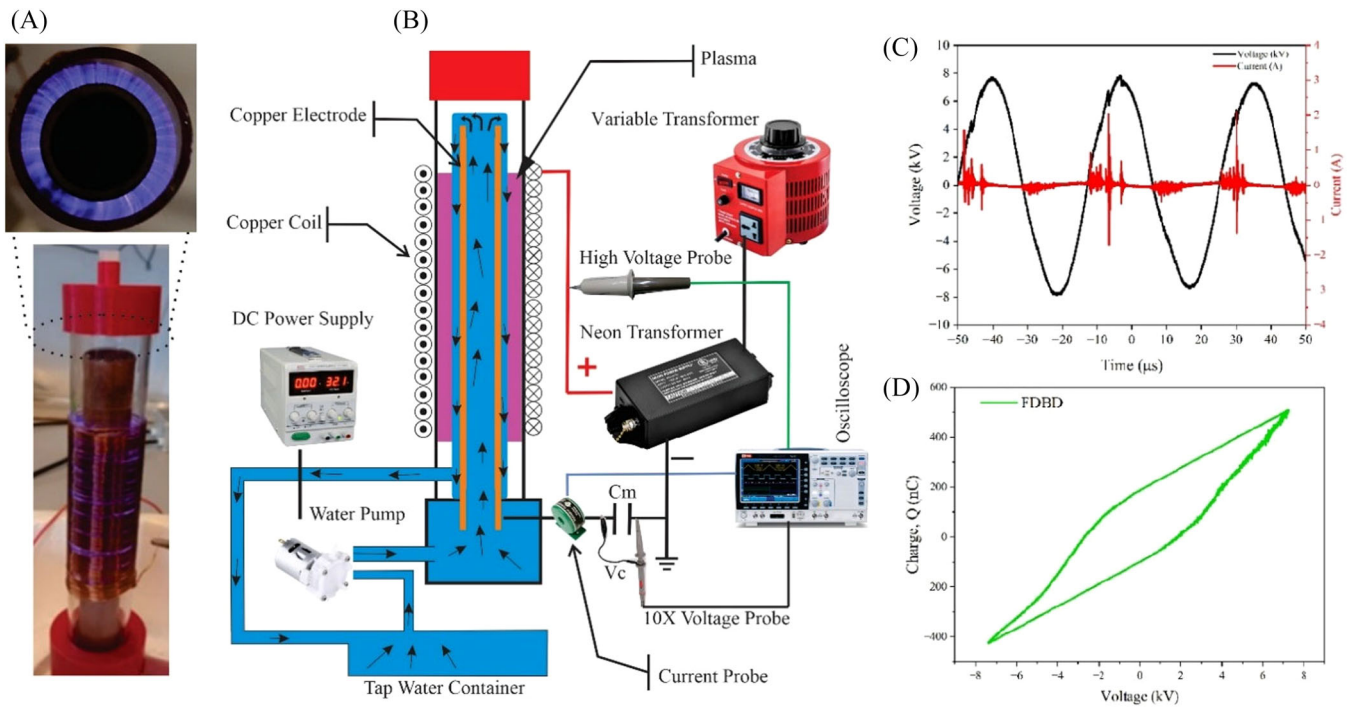


FIGURE 2 | Fountain dielectric barrier discharge, (A) real photograph, (B) schematic diagram, (C) voltage and current waveforms, and (D) Lissajous figure.

2.1.2 | Fountain Dielectric Barrier Discharge (FDBD)

Figure 2A,B shows real and schematic diagram of FDBD reactor and water circulating system, respectively. The same

reactor has been used previously in Kooshki et al. [30]. An AC neon transformer (15 kV, 20 kHz) and a variable transformer are used for generating plasma. A DC power supply was used for the water pump. The reactor is suitable to treat

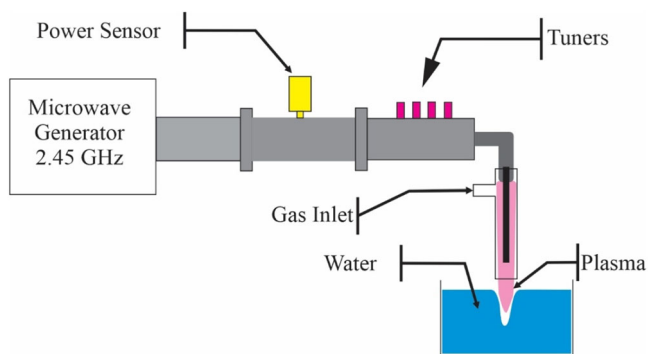


FIGURE 3 | Schematic of microwave plasma setup in Proline Solutions company (Austria).

a large volume of water with a typical 85 mL/min flow rate. The reactor is shaped like a coaxial cylinder, and the dielectric is a quartz tube that is 180 × 25 mm in size with 1.5 mm thickness. The central tube electrode is made of copper, and at the outer surface, a copper coil is wrapped around the glass dielectric. The spacing between the inner and outer tubes (discharge gap) is 3 mm. After being fed into the reactor, water flows laminarly upwards through the central Cu tube before dropping out the top of the central tube into the gap with a micro discharge zone. One liter of water was treated for 20 min. Figure 2C shows the current–voltage waveform of the FDBD. We used the Lissajous figure method to measure the dissipated power. To measure the charge that was transferred during plasma discharge, a reference capacitor ($C_m = 6$ nF) was placed in series with the FDBD device. The voltage across the FDBD electrodes and the voltage across the measurement capacitor were simultaneously recorded using the high-voltage probes and a digital oscilloscope. The charge Q was calculated from the voltage across the capacitor using the relation $Q = C_m V_C$. A Lissajous figure was plotted by DBD voltage (x -axis) against the calculated charge (y -axis) over one full AC cycle. The area enclosed by the resulting figure corresponds to the energy dissipated per cycle (Figure 2D), which corresponds to the discharge power of 48.8 W.

2.1.3 | Microwave (MW) Plasma

The water activated by MW plasma is prepared by *Proline Solutions* company (Austria). The MW power supply operates at a frequency of 2.45 GHz. Schematic diagram of the MW plasma is shown in Figure 3. The plasma system consumes 1.8 kW of electrical power and produces 45 L of PAW/h. More details of the MW PAW are specified in reference [31].

2.2 | Plasma-Activated Water Analysis

2.2.1 | Physiochemical Parameters of PAW

The pH and ORP are measured using a portable meter (WTW 3110, Weilheim, Germany). EC and temperature are measured with a digital conductivity meter (GMH 3430, GREISINGER

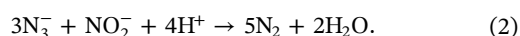
electronic, Germany). TDS is measured by 4-in-1 Multi Meter (Noyafa Digital, Philippines).

2.2.2 | Hydrogen Peroxide and Ozone Measurements

The quantity of H_2O_2 in PAW was measured by its interaction with titanyl ions from titanium oxysulfate ($TiOSO_4$), yielding a yellow product of pertitanic acid with a maximum absorbance peak at 407 nm [32]:



UV-VIS spectrometer (Shimadzu 1900) is used for detecting the absorption spectra. The yellow-colored compound generated is stable for a minimum of 6 h. To counteract the decomposition of H_2O_2 by the reaction with nitrites in PAW, a 60-mM solution of sodium azide (NaN_3) is included into the samples containing H_2O_2 prior to their mixing with $TiOSO_4$ reagent. Sodium azide promptly converts nitrites into molecular nitrogen under acidic conditions.



After the combination of the samples with azide, we add the titanium oxysulfate reagent into the sample. The $TiOSO_4$ to the sample ratio is 2:1.

We used the indigo colorimetric technique using indigo blue reagent to detect the quantity of dissolved ozone in PAW [33]. This method relies on the fast and precise interaction between ozone and indigo blue dye in an acidic environment, leading to the degradation of the indigo blue molecular structure, which causes the dye to fade or bleach. The bleaching action results in a quantifiable reduction of the peak absorbance of indigo blue at 600 nm. The extent of the absorbance reduction is directly proportional to the concentration of ozone in the sample. Consequently, by quantifying the variation in absorbance using a UV-Vis spectrophotometer (Shimadzu 1900), the quantity of dissolved ozone can be precisely determined.

2.2.3 | Nitrite and Nitrate Measurements

Nitrite NO_2^- was quantified using a commercial kit containing Griess reagent (Cayman Chemicals, Ann Arbor, MI, USA), resulting in a pink azo-product with a maximal absorbance peak at 540 nm [34]. The NO_2^- concentration in PAW is proportional to this absorbance and is calculated from the calibration curve.

For nitrate NO_3^- measurement in PAW, we used 2,6-dimethylphenol (DMP) (Sigma-Aldrich, USA) that with nitrate in sulfuric and phosphoric acid solution reacts to form 4-nitro-2,6-dimethylphenol that is spectrophotometrically detected at ~330 nm [35]. The NO_3^- concentration in PAW is proportional to this absorbance and is calculated from the calibration curve. However, when PAW contains both NO_2^- and NO_3^- , the DMP chemical probe is also sensitive to NO_2^- , hence careful measurement of NO_2^- by the Griess reagent and its subtraction from the DMP absorbance was applied.

2.3 | Effect of PAW on Seeds and Plants

2.3.1 | Seed Germination Parameters

Lactuca sativa (*L. sativa*; hybrid Cassini) seeds were purchased from the regional agriculture market (Moravoseed, Slovakia). The germination experiments were performed in petri dishes using filter paper (KA 4, Czech Republic), we used two filter papers in each Petri dish. The seeds were divided into four experimental groups: tap water as the control, and PAW produced by TS, FDBD, and MW plasma. The samples were irrigated with 3 mL of PAW at 24-h intervals and incubated for 7 days. Each group consisted of 3 replicates (30 seeds each), and all three replicated experiments were conducted under identical experimental conditions to verify the repeatability of the results. The seeds were germinated in a controlled environment at a temperature of $23^{\circ}\text{C} \pm 2^{\circ}\text{C}$, for 24 h in darkness. Petri dishes were briefly exposed to ambient room light solely for counting of the germinated seeds (< 1 min). The number of germinated seeds was monitored and documented daily.

- Germination Percentage (GP)

GP is typically expressed as the percentage of seeds that successfully germinate out of the total number of planted seeds, over a specific period of time:

$$\text{GP} = \frac{N_g}{N_t} \times 100. \quad (3)$$

N_g is the quantity of germinated seeds, N_t is total number of seeds.

- Mean Germination Rate (MGR)

MGR is a measure that takes into account not just how many seeds germinate, but also the time it takes for the seeds to germinate. It provides a more comprehensive understanding of the germination process.

$$\text{MGT} = \frac{\sum(n \times t)}{\sum n} \quad (4)$$

where n is the number of seeds germinated at time t .

- Seedling Vigor Index (SVI)

The SVI of seedlings is a metric used to assess the general health, vigor, and potential for effective development of plant seedlings. It combines two essential elements:

$$\text{SVI} = \text{Germination percentage} \times \text{shoot length}. \quad (5)$$

- Richard's function

The effect of stressors on germination can be estimated by induced changes in parameters of germination kinetics, derived using Richard's function [36] applied for the analysis of the germination seed population [37]. This function was chosen over simpler models (e.g., logistic or Gompertz) due to its ability to represent asymmetric germination curves:

$$Y_t = \frac{a}{(1 + b \cdot d \cdot e^{-c \cdot t})^{1/d}} \quad (6)$$

where Y_t is the germination parameters; a , b , c , and d are fitting parameters; t is time. The parameter in the equation is determined based on the percentage of fully germinated seeds in the sample. The optimal value of parameters a , b , c , and d was selected by applying the nonlinear least squares method and the "Solver" in Microsoft Excel and goodness of fit (R^2) values were recorded for each treatment group. The indices of germination kinetics include the final GP (V_i), median germination (M_e), and quartile deviation (Q_u):

$$V_i = a; \quad (7)$$

$$M_e = \frac{1}{c} \cdot \ln \frac{b \cdot d}{2^d - 1}; \quad (8)$$

$$Q_u = \frac{1}{2c} \cdot \ln \frac{4^d - 1}{(4/3)^d - 1}; \quad (9)$$

$$S_k = 2 \cdot \left\{ \ln \frac{d}{2^d - 1} / \ln \frac{4^d - 1}{(4/3)^d - 1} \right\}. \quad (10)$$

The M_e is inversely related to the germination rate, meaning that a lower M_e value corresponds to a higher germination rate, as it signifies that half of the seeds have germinated in less time. The Q_u indicates the dispersion of germination time in a seed lot. S_k denotes the skewness in the frequency distribution of germination time. These parameters are calculated for control and treatment groups using the coefficients a , b , c , and d of Richard's functions.

2.3.2 | Physical Parameters of Plant Growth Experiments in Soil

The same *L. sativa* (hybrid Cassini) seeds from regional agriculture market (Moravoseed, Slovakia) were used for the experiments where the seeds were planted into pots with soil and allowed to grow. Over the course of 6 weeks, they were irrigated with PAW every 2–3 days. In total, 5 mL of PAW is used for irrigation before germination, 20 mL during the second and third weeks, and 30 mL during the fourth week. There were 8 seeds in each pot and 12 pots for each group. Each pot (8×8 cm) included 8 seeds spaced evenly to minimize competition. Although the density of seeds per pot is relatively high, the same setup was used across all treatment groups. This procedure was enough for short-term (6-week) early growth analyses, though it may not reflect optimal spacing for full development. This limitation is acknowledged when interpreting biomass-related results. Following 6 weeks of irrigation with the three types of PAW, a comprehensive assessment of visual characteristics (quantity and quality of leaves), plant height, plant growth metrics (fresh and dry weight of whole plant), germination rate in soil, and photosynthetic pigments (chlorophyll $a + b$) content in both the above-ground parts and roots of lettuce plants were conducted. In this experiment, the pots with plants were located at a west-oriented window at room temperature (20°C) and $\sim 16/8$ daylight/night cycle (with ~ 7 h of direct sunlight daily in average).

2.3.3 | Photosynthetic Pigment Concentration Measurement

Lichtenthaler's method [38] was used to determine the concentration of photosynthetic pigments in leaves, namely chlorophylls a and b and carotenoids. The samples of lettuce leaves tissue are homogenized with 2 mL of 80% ethanol and centrifuged at 14 000g for 15 min. The supernatant was adjusted to a certain amount and diluted to achieve a linear absorbance range of 0.3–0.7. The concentrations of chlorophyll a, chlorophyll b, and carotenoids (xanthophylls and carotenes, x + c) were assessed based on absorbance readings obtained from a UV–VIS spectrophotometer (Shimadzu 1900, Japan) at wavelengths of 664, 648, and 470 nm, respectively. Three samples from each treatment were collected in every experimental trial.

2.4 | Statistics

The results are presented using mean values \pm standard deviation. A one-way analysis of variance (ANOVA) and subsequent multiple range test using the least significant difference technique were conducted to assess the differences across the groups. The various lowercase letters indicate a statistically significant difference at a probability level of $p < 0.05$.

3 | Results and Discussion

3.1 | PAW Characterization

PAW serves as a reservoir of various RONS, which have been shown to enhance the plant growth under stress conditions while also offering a potential alternative to conventional fertilizers. The priming effect of hydrogen peroxide (H_2O_2) on seeds plays a crucial role in accelerating and amplifying plant responses to environmental stressors [39]. Additionally, nitrate (NO_3^-) and nitrite (NO_2^-) present in PAW contribute as essential nitrogen sources required for the synthesis of proteins and other macromolecules, in addition to their signaling function. Several studies suggest that PAW can act as an alternative to chemical biostimulants, particularly in early plant developmental stages, such as seed germination [40]. However, the effectiveness of PAW is influenced by multiple factors, including the plant species, the specific chemical composition of PAW, and the experimental conditions under which PAW is applied [41].

Characteristics of tap water (control) and the three PAW types are shown in Table 1. A little reduction in pH was observed between the control and TS PAW, as well as FDBD; however, for MW PAW, pH was as low as 3.9. The little pH variation before and after plasma treatment may be attributed to the inherent hydrogen carbonate and bicarbonate buffer system in tap water, in contrast to the significant acidification reported during plasma treatments of deionized or distilled water [42, 43]. Our prior papers also confirmed these minor pH variations using tap water [18, 44, 45]. Overall pH changes were minimal in TS and FDBD, rendering this parameter a nondisruptive element in the germination process.

The EC and TDS increased after activation by plasma for all PAWs which is due to the formation and transport of active species and ions from plasma to PAW. Many previous works confirm this effect [46, 47]. ORP is an indicator that illustrates the propensity of a solution to become an oxidizing or reducing agent. As shown in Table 1, ORP of PAW increases after plasma treatment. Although TS-PAW exhibited the highest H_2O_2 concentration, its ORP remained relatively low. This is likely due to the near-neutral pH (~ 7.4), which reduces the oxidative contribution of H_2O_2 , as its redox potential is pH-dependent. Additionally, the presence of reducing species such as NO_2^- may also offset the oxidative strength. In contrast, MW-PAW showed a significantly higher ORP despite lower H_2O_2 levels, mainly due to its strong acidification and high NO_3^- concentration. This highlights that ORP reflects the combined effect of multiple redox-active species and the solution pH. Although a slight temperature increase was shown right after plasma treatment, all PAWs were isothermal with the ambient environment before irrigation. The discharge power was adjusted to 52.5 W (21×2.5 W) for the TS plasma, 48.8 W for the FDBD plasma, and 1800 W for the MW plasma, with different volumes of water used in each case according to the plasma system configuration.

Figure 4 illustrates the concentrations of H_2O_2 , O_3 , NO_2^- , and NO_3^- produced in the three types of PAW. The concentrations of H_2O_2 obtained were around 479 μM , 51 μM , and 3 μM for TS, FDBD, and MW, respectively. The O_3 values for TS, FDBD, and MW PAW were only 6.7 μM , 2.7 μM , and 0.1 μM , respectively. The NO_2^- values for TS, FDBD, and MW were around 1.32 mM, 0.26 mM, and 0.11 mM, respectively. The NO_3^- values for TS, FDBD, and MW were around 1.94 mM, 0.93 mM, and 6.91 mM, respectively. All plasma sources are abundant sources of RONS transported into water, as previously shown [18, 44, 45, 48]. The almost stable pH (in TS and FDBD) ensures that these RONS

TABLE 1 | Physicochemical properties of PAW prepared using three plasma systems: transient spark (TS), fountain dielectric barrier discharge (FDBD), and microwave (MW) plasma.

	pH	EC ($\mu\text{S}/\text{cm}$)	ORP (mV)	TDS (ppm)	Temp ($^{\circ}\text{C}$)	Power (W)
TW	7.7 ± 0.2	538.5 ± 8.5	250 ± 24	290.5 ± 3.5	21.3 ± 1.3	—
TS	7.41 ± 0.30	582.5 ± 3.5	286.7 ± 17.3	334.5 ± 2.5	26.3 ± 0.75	52.5
FDBD	7.35 ± 0.25	569 ± 3	261.05 ± 37	312 ± 11	24.0 ± 0.25	48.8
MW	3.95 ± 0.05	747.5 ± 10.5	402.9 ± 23.2	409 ± 4.9	23.0 ± 0.3	1800

Note: Tap water (TW) served as the untreated control. Values represent mean \pm SD ($n = 6$) from independent preparations. No statistical comparison was applied due to the use of different plasma systems.

Abbreviations: EC, electrical conductivity; ORP, oxidation–reduction potential; TDS, total dissolved solids; Temp, temperature.

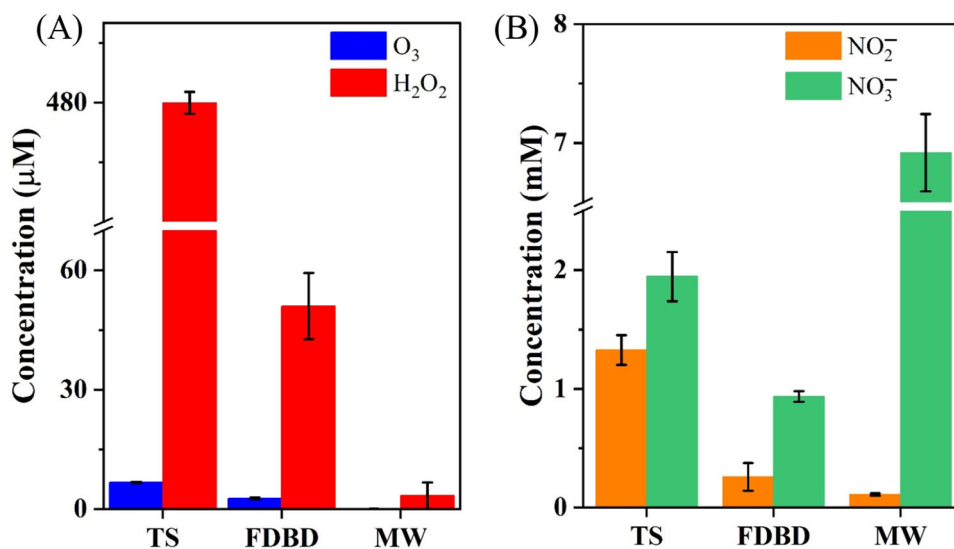


FIGURE 4 | Concentrations of H_2O_2 , O_3 (A), NO_2^- , and NO_3^- (B), in plasma-activated water produced by TS, FDBD, and MW plasma. Values are presented as a mean \pm standard deviation ($n = 6$).

remain intact for many hours postplasma treatment, hence enhancing their applicability to plants, except for MW where pH was reduced to 3.9. The TS and FDBD PAW are similar in composition, but TS PAW shows higher concentrations of all species, while MW makes dominantly an acidic solution of NO_3^- .

3.2 | Seed Germination in Petri Dishes

Figure 5A,B shows the variations in Germination Percentages (GP) and Mean Germination Time (MGT) caused by various PAW. Although GP and MGT for MW PAW is higher, there is no significant difference between data. Figure 5C illustrates the impact of PAW on seed vigor. The PAW has a significant effect on the vigor of the seeds. All groups showed significant differences compared to Tap water.

Dobrin et al. [49] reported that ROS induced by PAW may lead to seed coat cracking and thinning, thereby enhancing water and nutrient uptake. This process has been associated with improved germination parameters, including a higher germination rate, germination index, and vigor index. However, in our study, different PAW treatments did not significantly affect the percentage of germinated seeds or the MGT. Notably, significant changes were observed in the seed vigor index which reflects seed quality and energetic potential during germination and early growth stages.

Figure 6 illustrates the impact of PAW on the shoot and root lengths of *L. sativa* L. seedlings on Day 8. The shoot and root exhibited different responses to PAW treatment. A visual comparison of root morphology reveals that the root length was reduced in PAW-treated seedlings compared to those irrigated with tap water (hypocotyl necks are shown in Figure 6). However, the root length was not a determining factor for the growth and quality of leafy plants. During germination, seeds rely on their internal nutrient stores to support the embryo growth, which may explain the limited PAW effect on root elongation.

In contrast, shoot length showed a significant increase across all three PAW treatments. Seedlings treated with TS, FDBD, and MW PAW exhibited shoot length increases of 14.3%, 21.7%, and 22.5%, respectively, compared to the control.

Figure 7A compares the average shoot and root length of plant and a level of difference between data. Figure 7B shows the number of seedlings longer than 3 cm (upper part), which was shown to be most impacted by MW PAW, followed by TS, and then FDBD PAW. During the germination stage, seedlings need additional external nutrition for optimal plant growth. In PAW, NO_3^- functions both as a signaling molecule and a chemical that may indirectly provide nutrients to seedlings. Consequently, the seedlings in all PAW samples exhibit superior growth indices relative to the tap water.

The germinating data were well adapted to the Richard's function (Figure 8). The Richard's function indicates that MW and FDBD exhibited a smoother initial phase of germination. All treatments reached their maximum germination rate on the 2nd and 3rd days. Population parameters V_i (viability), M_e (median germination time), Q_u (dispersion) and SK (skewness) of the Richard's function are shown in Table 2.

Analysis of Richard's function parameters showed no statistically significant differences in final viability among treatments. When analyzing the germination results (Table 2), the FDBD treatment showed the highest seed viability (97.06%) and the shortest median germination time ($M_e = 1.41$ days), suggesting improved germination dynamics compared to other treatments. However, these differences were not statistically significant ($p > 0.05$), as indicated by shared superscript letters.

Among the treatments, seeds irrigated with MW PAW exhibited germination parameters comparable to those of the other plasma treatments, with a trend toward a smoother initial germination phase. These responses were associated with PAW containing the highest initial concentration of NO_3^- and minimal concentrations of O_3 and H_2O_2 . In contrast, TS and FDBD

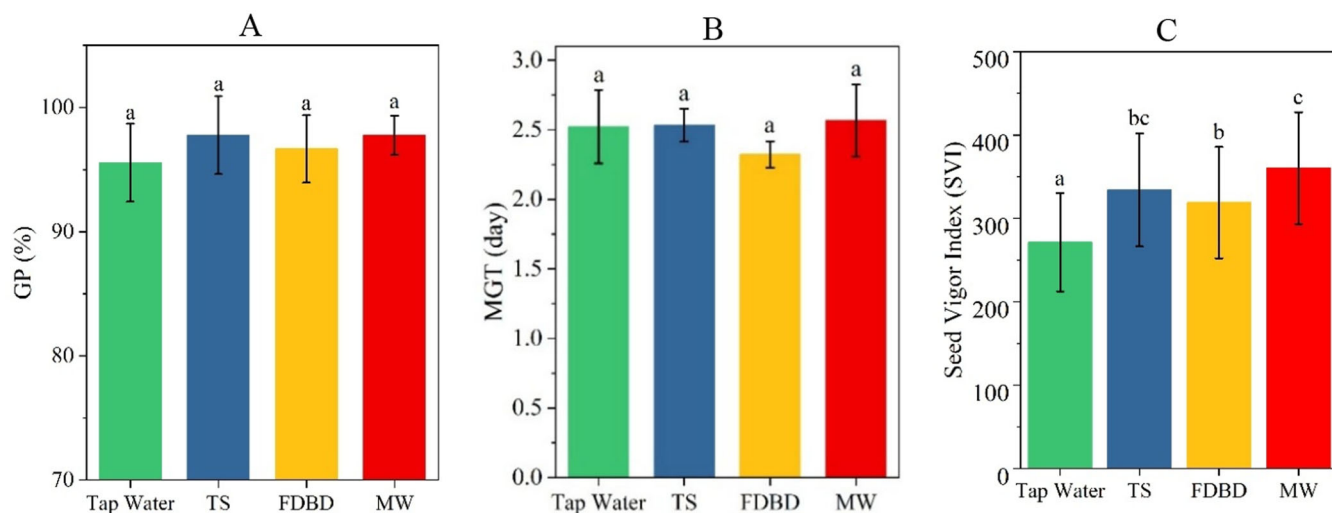


FIGURE 5 | Seed germination parameters (A) GP, (B) MGT, and (C) SVI. Values are presented as a mean \pm standard deviation ($n = 3$). Different lowercase letters indicate significant differences among the treatments at $p < 0.05$.

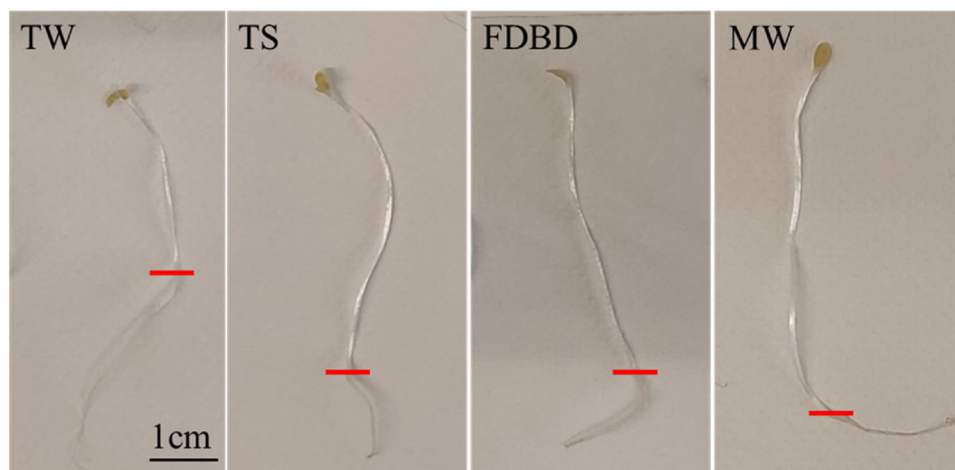


FIGURE 6 | Photographs of seedlings germinated 8 days after being sown. Red lines show transitions between the root and the hypocotyl. Scale bar 1 cm.

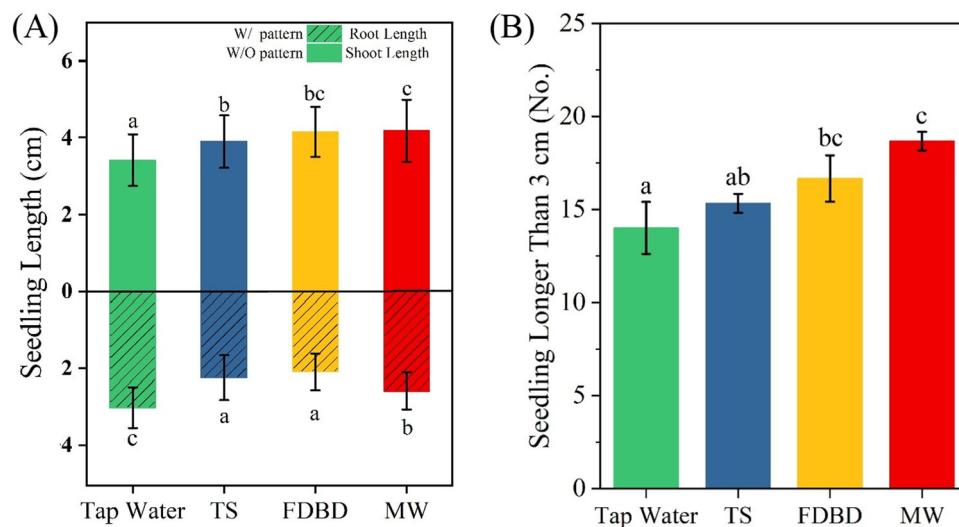


FIGURE 7 | (A) Seedling length on 8th day after sowing. (B) Number of seedlings longer than 3 cm. Values are presented as a mean \pm standard deviation ($n = 3$). Different lowercase letters indicate significant differences among the treatments at $p < 0.05$.

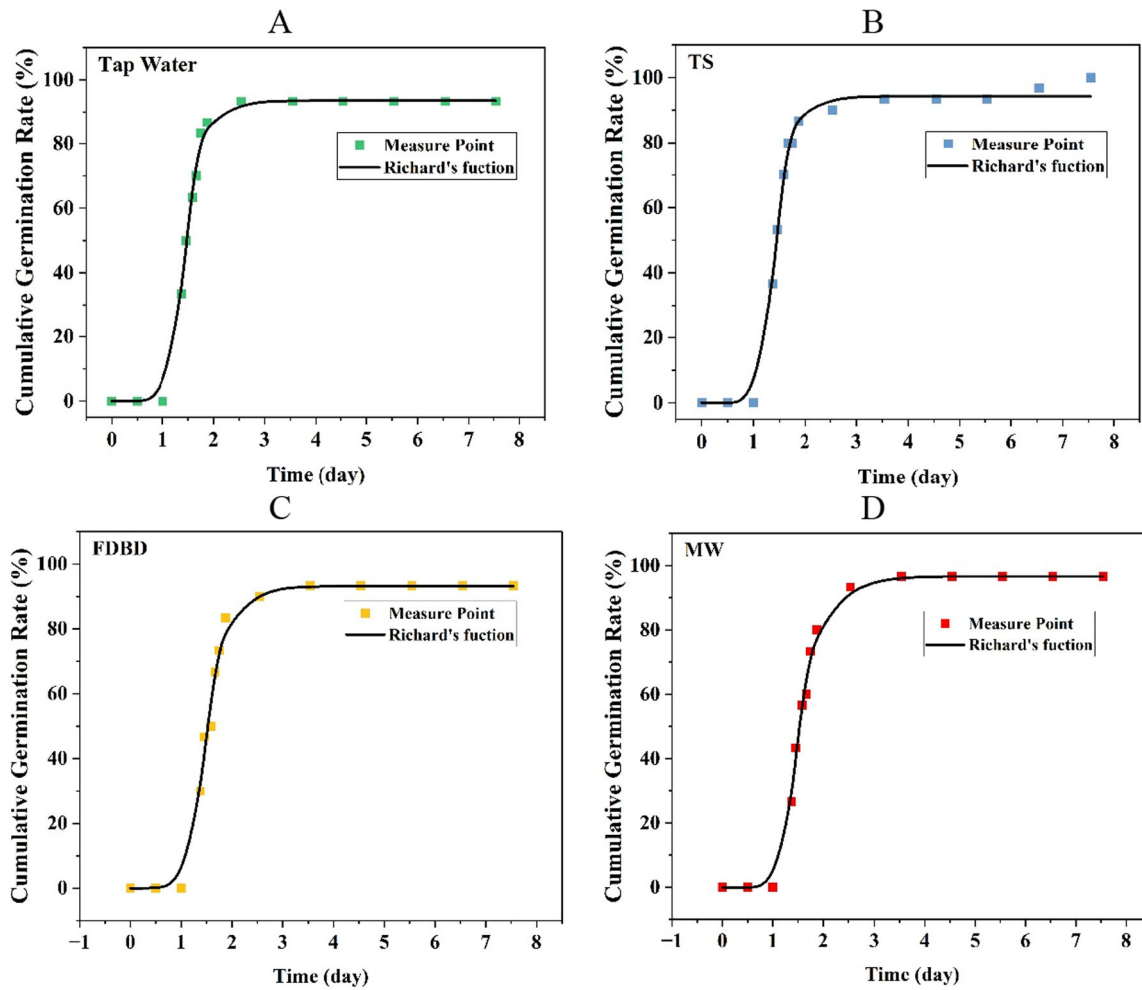


FIGURE 8 | Richard's function fitted to the germination of lettuce seeds treated by (A) tap water, (B) TS, (C) FDBD, and (D) MW.

TABLE 2 | The Richard's function for germination's population characteristics: V_i (viability), M_e (median germination time), Q_u (dispersion), and S_k (skewness).

Treatment group	V_i (%)	Q_u (day)	M_e (day)	S_k	R^2 value
TW	92.29 ± 2.87^a	0.184 ± 0.037^a	1.49 ± 0.032^a	0.484 ± 0.49^a	0.99
FDBD	96.04 ± 3.38^a	0.199 ± 0.027^a	1.41 ± 0.0775^a	0.456 ± 0.03^a	0.98
TS	96.044 ± 5.38^a	0.152 ± 0.0173^a	1.46 ± 0.026^a	0.576 ± 0.321^a	0.95
MW	95.56 ± 3.51^a	0.187 ± 0.016^a	1.46 ± 0.079^a	0.46 ± 0.349^a	0.99

Note: Values are presented as a mean \pm standard deviation ($n = 3$). Superscript indices: different lowercase letters indicate statistically significant differences among the treatments at $p < 0.05$.

produced markedly higher levels of H_2O_2 and moderate amounts of O_3 , yet germination parameters remained statistically similar to the control. This suggests that while plasma treatments did not significantly alter GP or speed, the chemical composition of PAW may contribute to subtle differences in seedling vigor. Similar positive effects of PAW have been reported in previous studies. For instance, in 2011, Neumanová et al. [50] observed a 1.5-fold increase in coleoptile length in rye seedlings treated with PAW compared to untreated controls. Furthermore, Kučerová et al. [40] found that during the early growth stages, seeds primarily interact with H_2O_2 during imbibition and germination, whereas NO_3^- and NO_2^- are metabolized later, following germination initiation. The

relatively low concentration of H_2O_2 in MW PAW may therefore have been beneficial, as H_2O_2 at low levels acts as a signaling molecule activating antioxidant defenses, while excessive levels—as in TS PAW—could become cytotoxic and hinder growth [51].

3.3 | Seed Germination and Plant Growth in Soil

Lettuce seeds were planted and germinated directly in the pots with soil and were watered with PAW during 6 weeks, every 2–3 days: before germination 5 mL in each pot, second and third weeks 20 mL per pot and in the fourth week to last week

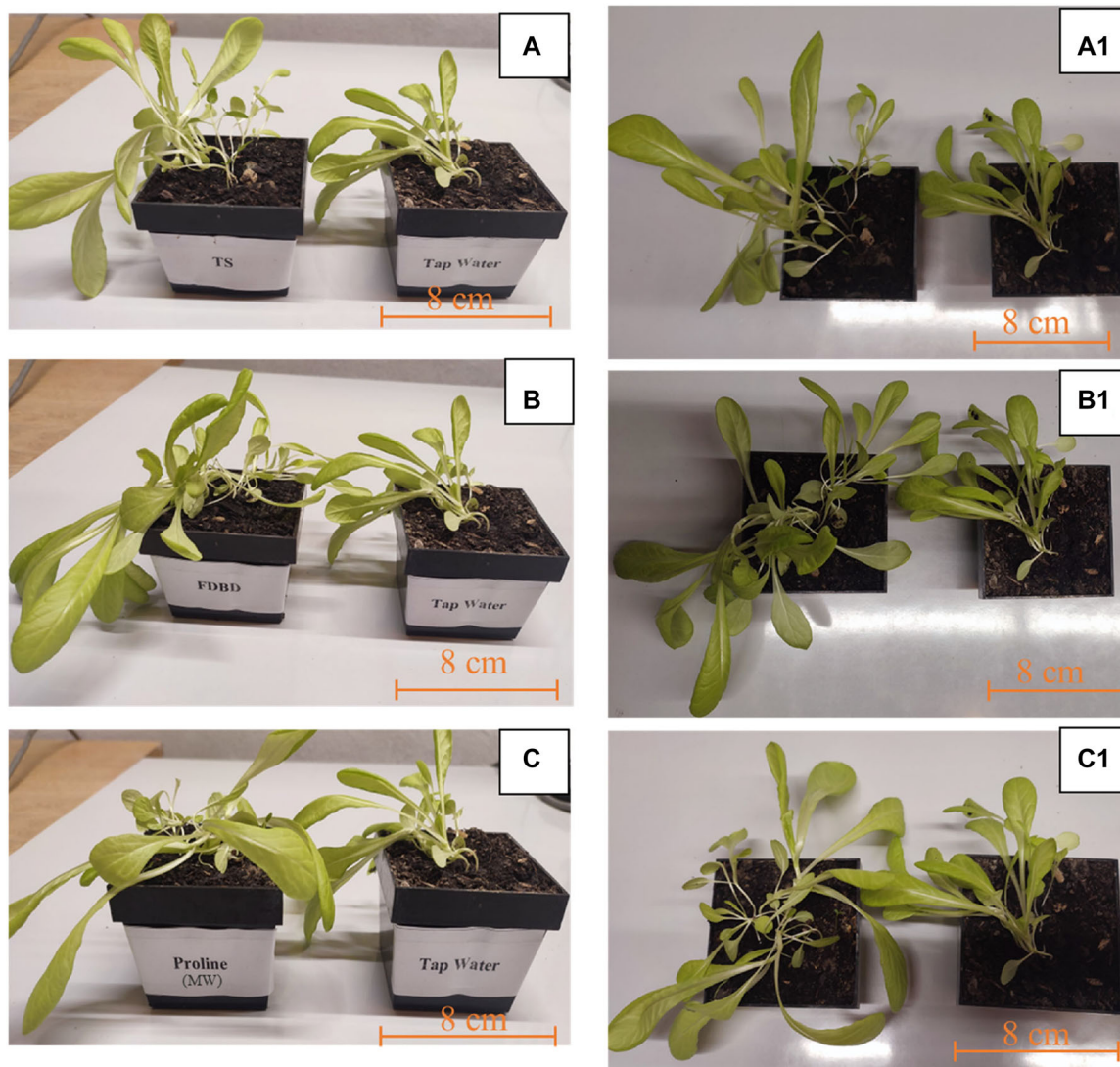


FIGURE 9 | Photographs of lettuce plants after 4 weeks of cultivation in soil watered with tap water (control) and PAW. TS and tap water (A), FDBD and tap water (B), MW and tap water (C). (A–C) Front view, (A1–C1) top-down view. Scale bar 8 cm.

30 mL of PAW per pot was used for irrigation. The PAW-irrigated plants exhibited considerably greater leaf sizes in comparison to the control, as demonstrated in Figure 9.

The morphological characteristics of the plants, including the leaf dimensions, quantity, and developmental stage, were evaluated to assess the effects of PAW on plant growth. The results indicate that lettuce plants irrigated with PAW exhibited considerably greater biomass accumulation compared to the control tap water irrigation. This enhancement in growth parameters suggests that PAW contributes to improved nutrient availability and physiological responses in plants.

As shown in Figure 10A, there is no significant difference in germination rate of seeds within 7 days after sowing into soil. While there is no difference in the quantity of leaves (for each pot) for MW-activated water (2%), we observed a 20% increase in the leaf quantity in TS and FDBD groups which is shown in Figure 10B.

There is an increase in the plant length of ~25% for FDBD and slightly above 30% equally for TS and MW compared with

control (Figure 10C). The dry weight more accurately represents the changes in biomass. The fresh and dry weights of the above-ground parts and roots of lettuce exhibited similar tendencies. Figure 10D,E shows 1.1, 1.15, 1.31-fold increase in the fresh weight, and 1.28, 1.35, 1.62-fold increase in the dry weight of plant when TS, FDBD, and MW PAW were used for irrigation, respectively.

There is no significant difference in root length for TS with respect to control, but 1.59- and 1.28-fold increase showed by FDBD and MW. In addition, plant root volumes in MW and FDBD are higher in comparison TS and Control, as shown in Figures 10F and 11 specifically shows photographs of the roots of the representative plants in each experimental group.

Nitrate (NO_3^-) is a key macronutrient, serving as the primary nitrogen source for plant growth while also functioning as a signaling molecule that regulates gene expression involved in nitrogen transport and assimilation [52]. Efficient nitrogen uptake is crucial for optimizing photosynthesis, metabolic activity, and overall biomass production. Our findings

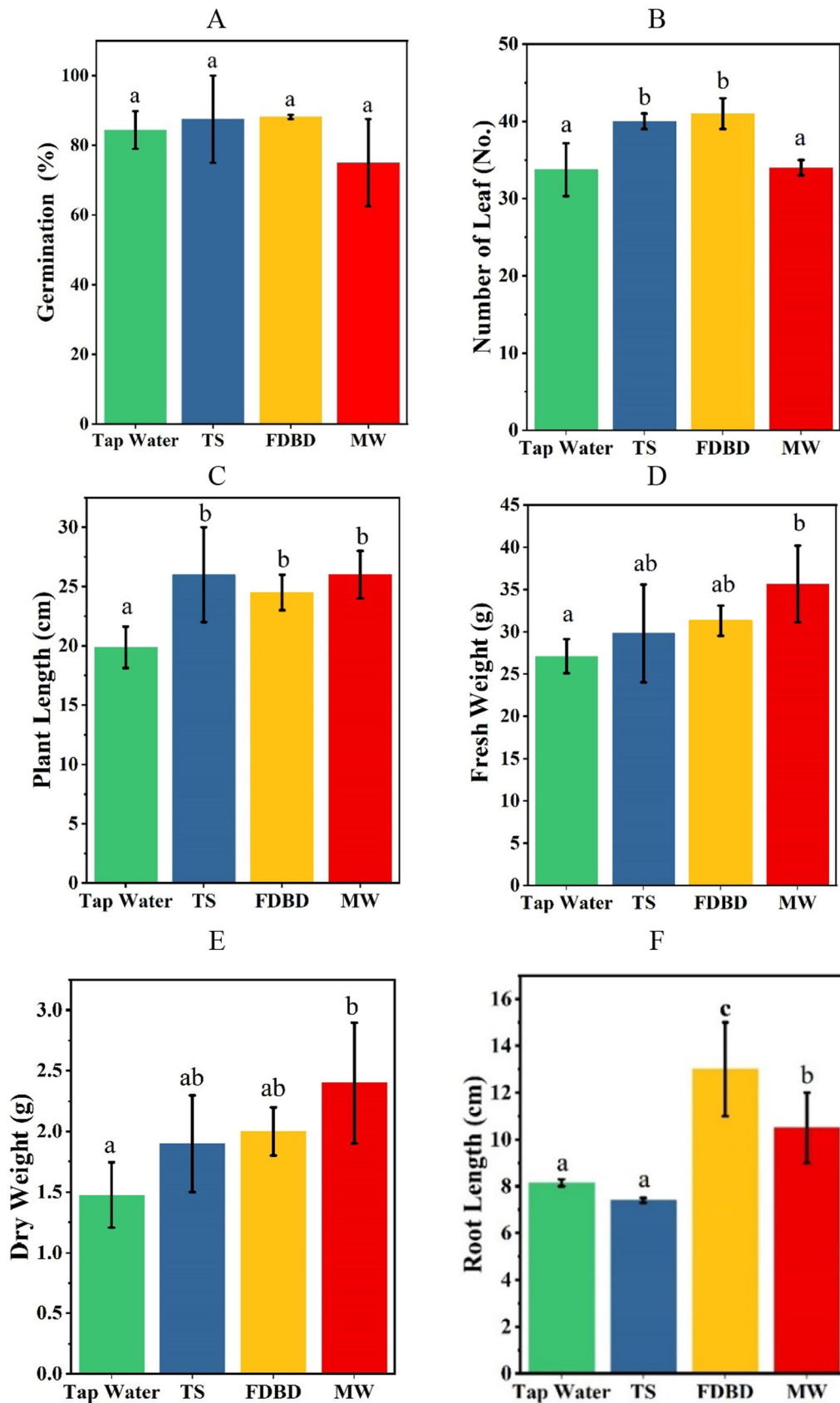


FIGURE 10 | Plant growth parameters (A) germination, (B) number of leaves, (C) plant length, (D) fresh weight 6 weeks after sowing, (E) dry weight 8 weeks after harvesting, and (F) root length. Values are shown as a mean \pm standard deviation ($n = 12$). Different lowercase letters indicate significant differences among the treatments at $p < 0.05$.

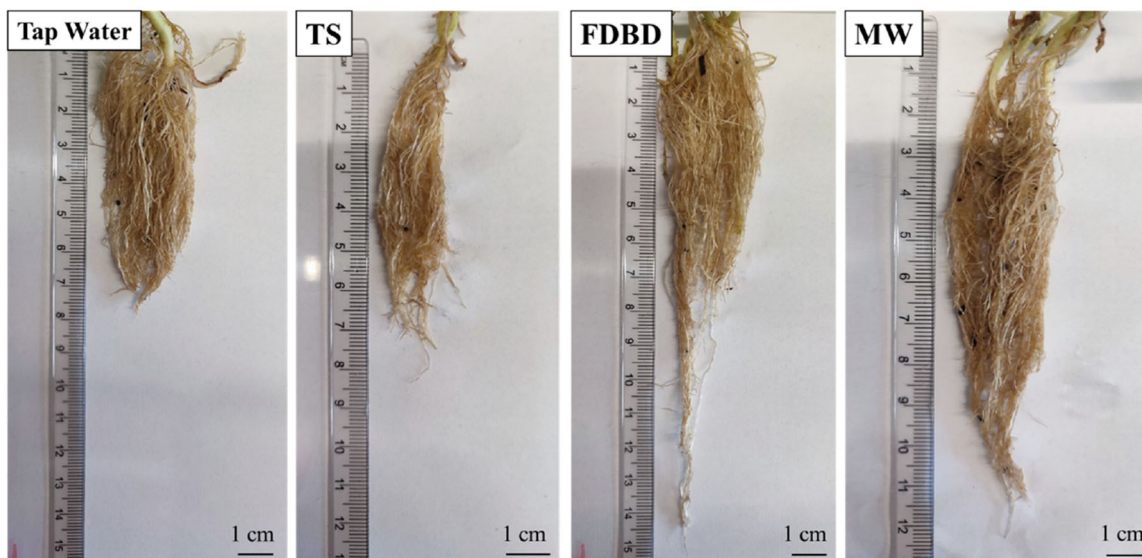


FIGURE 11 | Root length of the harvested plant after 6 weeks in soil. Scale bar 1 cm.

demonstrate a strong correlation between nitrate concentration and plant growth, supported by Pearson's correlation coefficient of $r = +0.982$ for nitrate versus fresh weight (FW) and $r = +0.996$ for nitrate versus dry weight (DW). Among all treatments, only plants watered with MW PAW have shown a statistically significant enhancement in both fresh and dry weight, correlating with the highest NO_3^- concentration recorded in this PAW. This suggests that MW-PAW irrigated plants not only benefited from enhanced nitrate availability but also exhibited greater water retention capacity, as indicated by the observed FW–DW ratio.

Nitrate availability, irrespective of its source—traditional nutrient solutions or PAW nitrate – significantly influences the key growth parameters, including plant height, root length, number of leaves, photosynthetic rate, and biomass production.

Interestingly, the TS and FDBD treatments were characterized by elevated H_2O_2 concentrations, which may have contributed to the improved growth. At low concentrations, H_2O_2 functions as a signaling molecule, activating antioxidant defense mechanisms that enhance the plant growth. Our results suggest that the H_2O_2 concentrations used in this study, ranging from sub-micromolar levels in MW PAW to nearly 0.5 mM in TS PAW, had a stimulatory effect on the monitored growth parameters. Similar findings have been reported by previous studies in various plant species, including spinach, pepper, tomato, soybean, mung bean [26, 53–56], as well as in the model plant *Arabidopsis thaliana* [57]. The positive effects of PAW treatment on biomass accumulation may be attributed to enhanced protein synthesis [41].

NO_3^- serves as the primary nitrogen supply for plant synthesis of proteins and nucleic acids; hence, it is regarded as the principal element of the PAW that contributes to biomass enhancement. Furthermore, H_2O_2 may contribute to biomass increases by promoting lignification of plant tissues. H_2O_2 enhances the activities of key enzymes involved in the phenylpropanoid pathway, including phenylalanine ammonia-lyase (PAL), cinnamate 4-hydroxylase (C4H), and 4-coumarate-CoA

ligase (4CL), leading to lignin accumulation. Additionally, H_2O_2 upregulates the activities of DNase, RNase, and caspase-3-like enzymes, which facilitate rapid lignification [58]. Moreover, H_2O_2 serves as a co-substrate in oxidation reactions during lignin polymerization, further reinforcing its role in structural reinforcement and biomass enhancement [59].

The quantity of photosynthetic pigments, that is, chlorophyll a, increased by 7% in plants irrigated by FDBD-treated water as shown in Figure 12A without pattern. Chlorophyll b was higher by 13% and 30% in plants irrigated with TS and FDBD PAW compared to control as shown in Figure 12A with pattern. Even though these differences were statistically significant ($p < 0.05$), the magnitude of the change suggests that it had a small effect on pigment biosynthesis rather than a major impact. However, the MW-treated water shows no significant difference in chlorophylls (Figure 12A). TS and FDBD results show about 1.5-fold increase in carotenoids with respect to the control, while the MW-treated water did not significantly increase carotenoids (Figure 12B).

Chlorophyll pigment content also indirectly provides information on mineral nutrition, as chlorophyll stores significant amounts of nitrogen. It is also a sign of overall plant metabolism [60, 61].

Investigating the effects of three different types of PAW on lettuce plants showed no significant impact on the production of photosynthetic pigment chlorophyll a. However, a significant difference in both chlorophyll b concentration and carotenoid synthesis was observed only under FDBD treatment. Carotenoids defend plants against photo-oxidation and have an additive function in photosynthesis. Their rise often signifies a rise in oxidative stress inside plant cells, which was higher in TS and FDBD PAW, since they had higher H_2O_2 concentrations [62].

Although H_2O_2 and O_3 concentrations were the highest in the TS treatment, this variant also exhibited elevated levels of NO_2^- and NO_3^- , which might serve as protective factors, mitigating the negative effects of H_2O_2 . Conversely, in the FDBD

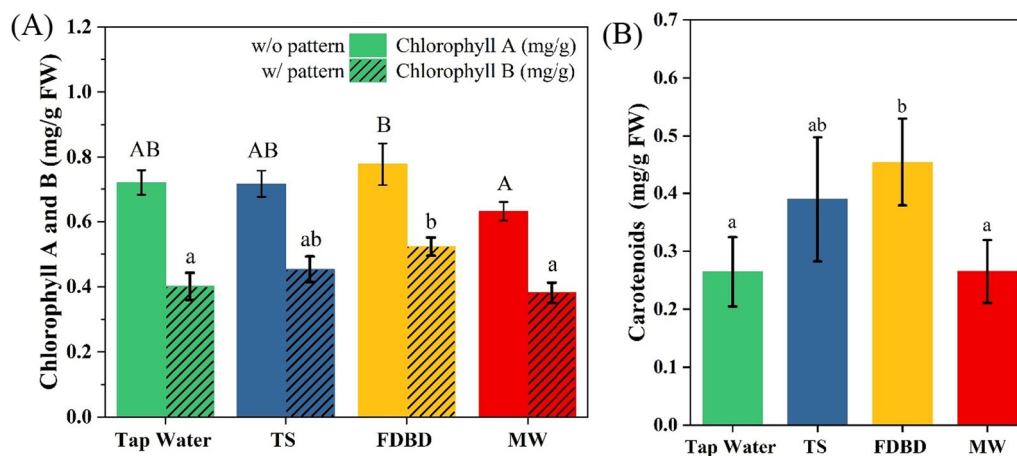


FIGURE 12 | (A) Chlorophyll A and B of FW, without (w/o) and with (w/) pattern, respectively. (B) Carotenoids content in above-ground parts of lettuce plants after 6 weeks of soil cultivation irrigated with the PAW. Values are presented as a mean \pm standard deviation ($n = 4$). Different letters indicate significant differences among the treatments at $p < 0.05$.

treatment, NO_2^- and NO_3^- concentrations were lower. Nitrate can also enhance the production of specific enzymes, such as peroxidases, which help neutralize H_2O_2 by converting it into water [63]. The lower availability of these anions in the FDBD treatment might limit these protective mechanisms, causing the plant to rely more on carotenoids as antioxidants. This suggests that the different effects of PAW treatments on oxidative stress response may be mediated by the availability of nitrogen species, influencing the balance between enzymatic and non-enzymatic antioxidant systems. While the uptake of RONS (e.g., NO_3^- , NO_2^- , H_2O_2) by plant tissues was not directly quantified, the identified correlations between PAW composition and plant responses indicate a biological effect mediated by these reactive species. Changes in the pH and EC of the water are important because they are caused by plasma-driven RONS formation (like the breakdown of nitric and nitrous acid). This means that they are an important part of the overall chemical profile of PAW. The synergistic effects of these species probably play a role in the stimulating effects seen in the plant growth.

Although we observed that certain PAW treatments with higher NO_3^- or H_2O_2 concentrations were associated with improved germination and growth parameters, these effects should be interpreted cautiously. Since each plasma system generates a unique mixture of RONS, causal attribution to individual species is speculative. Further studies involving isolation experiments or synthetic PAW mimics (e.g., controlled solutions of NO_3^- or H_2O_2) are needed to determine the specific contributions of individual reactive species to the observed plant responses. Further studies should also investigate the specific role of NO_3^- and NO_2^- in regulating peroxidase activity and how this interplay affects overall oxidative stress resilience in lettuce plants.

4 | Conclusion

The effect of PAW produced by three different plasma sources on germination parameters, visual appearance, growth parameters, and physiological and biochemical characteristics of *L.*

sativa seedlings germinated in petri dishes, and of 6-week-old plants cultivated in soil, were examined. Each air plasma source (TS, FDBD, and MW) produces different concentrations of RONS in PAW, which results in different effects on seedlings and plants. MW-PAW, which contained the highest nitrate levels but very low concentrations of H_2O_2 and ozone, resulted in the greatest improvements in fresh and dry biomass. This suggests that nitrate plays a key role as a nutrient and signaling molecule promoting biomass accumulation. In contrast, TS-PAW, with the highest H_2O_2 concentration and moderate nitrate levels, showed positive effects on shoot elongation and pigment accumulation, indicating that moderate levels of H_2O_2 may act as growth stimulants via redox signaling. However, our investigations indicate that PAWs have a negligible impact on lettuce seed germination parameters from petri dish germination.

These research results indicate that the impact of PAW on lettuce plants in soil surpasses that of germination and early seedling growth in petri dishes. Elevated amounts of RONS may be beneficial for some plant growth parameters; however, they might adversely affect others. This study findings indicate that PAW can favorably influence many physiological parameters of plants, especially increased nitrate promotes the plant growth and the total biomass. Nonetheless, the total impact of PAW on plant development in these experiments was rather limited, especially of TS and FDBD PAW that contained H_2O_2 . Consequently, the optimization of the PAW composition, as well as observation of plant growth over its entire life cycle are necessary steps before its final upscaling for agricultural use.

Acknowledgments

This study was funded by EU NextGenerationEU through the Recovery and Resilience Plan for Slovakia under the Project No. 09I03-03-V03-00033 EnvAdwice and the Slovak Research and Development Agency APVV-22-0247.

Conflicts of Interest

The authors declare no conflicts of interest.

Data Availability Statement

The data that support the findings of this study are available from the corresponding author upon reasonable request.

References

1. A. Sharma, "A Review on the Effect of Organic and Chemical Fertilizers on Plants," *International Journal for Research in Applied Science and Engineering Technology* 5, no. II (2017): 677–680, <https://doi.org/10.22214/ijraset.2017.2103>.
2. T. Sonoda, N. Takamura, D. Wang, T. Namihira, and H. Akiyama, "Growth Control of Leaf Lettuce Using Pulsed Electric Field," in *19th IEEE Pulsed Power Conference (PPC)* (2013), <https://doi.org/10.1109/PPC.2013.6627557>.
3. F. G. Reina, L. A. Pascual, and I. A. Fundora, "Influence of a Stationary Magnetic Field on Water Relations in Lettuce Seeds. Part II: Experimental Results," *Bioelectromagnetics* 22, no. 8 (December 2001): 596–602, <https://doi.org/10.1002/BEM.89>.
4. R. Mehrabifard, Z. Kabarkouhi, F. Rezaei, K. Hajisharifi, and H. Mehdian, "Physical Insight Into the Synergistic Enhancement of CAP Therapy Using Static Magnetic Field," *Brazilian Journal of Physics* 54, no. 4 (June 2024): 1–10, <https://doi.org/10.1007/S13538-024-01501-2>.
5. R. Mehrabifard, H. Mehdian, K. Hajisharifi, and E. Amini, "Improving Cold Atmospheric Pressure Plasma Efficacy on Breast Cancer Cells Control-Ability and Mortality Using Vitamin C and Static Magnetic Field," *Plasma Chemistry and Plasma Processing* 40, no. 2 (November 2020): 511–526, <https://doi.org/10.1007/s11090-019-10050-5>.
6. N. Puač, M. Gherardi, and M. Shiratani, "Plasma Agriculture: A Rapidly Emerging Field," *Plasma Processes and Polymers* 15, no. 2 (2018): 1700174, <https://doi.org/10.1002/ppap.201700174>.
7. C. Bradu, K. Kutasi, M. Magureanu, N. Puač, and S. Živković, "Reactive Nitrogen Species in Plasma-Activated Water: Generation, Chemistry and Application in Agriculture," *Journal of Physics D: Applied Physics* 53, no. 22 (2020): 223001, <https://doi.org/10.1088/1361-6463/ab795a>.
8. A. Mišúthová, Z. Lukačová, M. Ghulam, R. Mehrabifard, B. Šerá, and Z. Machala, "Effect of Plasma-Activated Water on Physiological Parameters in Bean Plants (*Phaseolus vulgaris*)," in *25th Symposium on Application of Plasma Processes* (February 2025), <https://doi.org/10.2139/SSRN.5137895>.
9. Z. Zhou, Y. Huang, S. Yang, and W. Chen, "Introduction of a New Atmospheric Pressure Plasma Device and Application on Tomato Seeds," *Agricultural Sciences* 2, no. 01 (2011): 23–27, <https://doi.org/10.4236/as.2011.21004>.
10. M. Henselová, L. Slovákova, M. Martinka, and A. Zahoranová, "Growth, Anatomy and Enzyme Activity Changes in Maize Roots Induced by Treatment of Seeds With Low-Temperature Plasma," *Biologia* 67, no. 3 (2012): 490–497, <https://doi.org/10.2478/s11756-012-0046-5>.
11. J. Pawlat, A. Starek, A. Sujak, M. Kwiatkowski, P. Terebun, and M. Budzeń, "Effects of Atmospheric Pressure Plasma Generated in Glidarc Reactor on *Lavatera thuringiaca* L. Seeds' Germination," *Plasma Processes and Polymers* 15, no. 2 (2018): 1700064, <https://doi.org/10.1002/ppap.201700064>.
12. A. Zahoranová, M. Henselová, D. Hudecová, et al., "Effect of Cold Atmospheric Pressure Plasma on the Wheat Seedlings Vigor and on the Inactivation of Microorganisms on the Seeds Surface," *Plasma Chemistry and Plasma Processing* 36, no. 2 (2016): 397–414, <https://doi.org/10.1007/s11090-015-9684-z>.
13. M. El Shaer, H. El Welily, A. Zaki, et al., "Germination of Wheat Seeds Exposed to Cold Atmospheric Plasma in Dry and Wet Plasma-Activated Water and Mist," *Plasma Medicine* 10, no. 1 (2020): 1–13, <https://doi.org/10.1615/PlasmaMed.2020033660>.
14. L. Sivachandiran and A. Khacef, "Enhanced Seed Germination and Plant Growth by Atmospheric Pressure Cold Air Plasma: Combined Effect of Seed and Water Treatment," *RSC Advances* 7, no. 4 (January 2017): 1822–1832, <https://doi.org/10.1039/c6ra24762h>.
15. M. Maniruzzaman, A. J. Sinclair, D. M. Cahill, X. Wang, and X. J. Dai, "Nitrate and Hydrogen Peroxide Generated in Water by Electrical Discharges Stimulate Wheat Seedling Growth," *Plasma Chemistry and Plasma Processing* 37, no. 5 (September 2017): 1393–1404, <https://doi.org/10.1007/S11090-017-9827-5/FIGURES/6>.
16. R. R. Zhou, J. Li, R. R. Zhou, X. Zhang, and S. Yang, "Atmospheric-Pressure Plasma Treated Water for Seed Germination and Seedling Growth of Mung Bean and Its Sterilization Effect on Mung Bean Sprouts," *Innovative Food Science & Emerging Technologies* 53 (May 2019): 36–44.
17. Y. M. Zhao, A. Patange, D. W. Sun, and B. Tiwari, "Plasma-Activated Water: Physicochemical Properties, Microbial Inactivation Mechanisms, Factors Influencing Antimicrobial Effectiveness, and Applications in the Food Industry," *Comprehensive Reviews in Food Science and Food Safety* 19, no. 6 (November 2020): 3951–3979, <https://doi.org/10.1111/1541-4337.12644>.
18. G. B. Ndiffo Yemeli, R. Švubová, D. Kostolani, S. Kyzek, and Z. Machala, "The Effect of Water Activated by Nonthermal Air Plasma on the Growth of Farm Plants: Case of Maize and Barley," *Plasma Processes and Polymers* 18, no. 1 (2021): 2000205, <https://doi.org/10.1002/PPAP.202000205>.
19. K. F. Sergeichev, N. A. Lukina, R. M. Sarimov, et al., "Physicochemical Properties of Pure Water Treated by Pure Argon Plasma Jet Generated by Microwave Discharge in Opened Atmosphere," *Frontiers in Physics* 8 (2021): 614684, <https://doi.org/10.3389/fphy.2020.614684>.
20. G. P. Bienert, J. K. Schjoerring, and T. P. Jahn, "Membrane Transport of Hydrogen Peroxide," *Biochimica et Biophysica Acta (BBA) – Biomembranes* 1758, no. 8 (August 2006): 994–1003, <https://doi.org/10.1016/J.BBAMEM.2006.02.015>.
21. B. G. Forde, "Nitrate Transporters in Plants: Structure, Function and Regulation," *Biochimica et Biophysica Acta (BBA) – Biomembranes* 1465, no. 1–2 (May 2000): 219–235, [https://doi.org/10.1016/S0005-2736\(00\)00140-1](https://doi.org/10.1016/S0005-2736(00)00140-1).
22. S. S. Goyal and R. C. Huffaker, "The Uptake of NO_3^- , NO_2^- , and NH_4^+ by Intact Wheat (*Triticum aestivum*) Seedlings: I. Induction and Kinetics of Transport Systems," *Plant Physiology* 82, no. 4 (December 1986): 1051–1056, <https://doi.org/10.1104/PP.82.4.1051>.
23. R. B. Lee, "The Effect of Nitrite on Root Growth of Barley and Maize," *New Phytologist* 83, no. 3 (November 1979): 615–622, <https://doi.org/10.1111/j.1469-8137.1979.tb02293.x>.
24. K. Gierczik, T. Vukušić, L. Kovács, et al., "Plasma-Activated Water to Improve the Stress Tolerance of Barley," *Plasma Processes and Polymers* 17, no. 3 (2020): 1900123, <https://doi.org/10.1002/PPAP.201900123>.
25. S. Zhang, A. Rousseau, and T. Dufour, "Promoting Lentil Germination and Stem Growth by Plasma Activated Tap Water, Demineralized Water and Liquid Fertilizer," *RSC Advances* 7, no. 50 (June 2017): 31244–31251, <https://doi.org/10.1039/c7ra04663d>.
26. L. Fan, X. Liu, Y. Ma, and Q. Xiang, "Effects of Plasma-Activated Water Treatment on Seed Germination and Growth of Mung Bean Sprouts," *Journal of Taibah University for Science* 14, no. 1 (January 2020): 823–830, <https://doi.org/10.1080/16583655.2020.1778326>.
27. R. Mentheour and Z. Machala, "Coupled Antibacterial Effects of Plasma-Activated Water and Pulsed Electric Field," *Frontiers in Physics* 10, no. July (2022): 1–15, <https://doi.org/10.3389/fphy.2022.895813>.
28. Z. Machala, M. Janda, K. Hensel, et al., "Emission Spectroscopy of Atmospheric Pressure Plasmas for Bio-Medical and Environmental Applications," *Journal of Molecular Spectroscopy* 243, no. 2 (2007): 194–201, <https://doi.org/10.1016/j.jms.2007.03.001>.

29. M. Janda, Z. Machala, A. Niklová, and V. Martišoviš, "The Streamer-to-Spark Transition in a Transient Spark: A dc-Driven Nanosecond-Pulsed Discharge in Atmospheric Air," *Plasma Sources Science and Technology* 21, no. 4 (2012): 045006, <https://doi.org/10.1088/0963-0252/21/4/045006>.
30. S. Kooshki, P. Pareek, M. Janda, and Z. Machala, "Selective Reactive Oxygen and Nitrogen Species Production in Plasma-Activated Water via Dielectric Barrier Discharge Reactor: An Innovative Method for Tuning and Its Impact on Dye Degradation," *Journal of Water Process Engineering* 63 (2024): 105477, <https://doi.org/10.1016/j.jwpe.2024.105477>.
31. Proline Solutions, "Proline Solutions – Just Another Astra Starter Templates Site," accessed February 4, 2025, <http://prolinesolutions.net/en/home-3/>.
32. G. Eisenberg, "Colorimetric Determination of Hydrogen Peroxide," *Industrial & Engineering Chemistry Analytical Edition* 15, no. 5 (1943): 327–328, <https://doi.org/10.1021/i560117a011>.
33. H. Bader and J. Hoigné, "Determination of Ozone in Water by the Indigo Method," *Water Research* 15, no. 4 (January 1981): 449–456, [https://doi.org/10.1016/0043-1354\(81\)90054-3](https://doi.org/10.1016/0043-1354(81)90054-3).
34. M. Moorcroft, "Detection and Determination of Nitrate and Nitrite: A Review," *Talanta* 54, no. 5 (2001): 785–803, [https://doi.org/10.1016/S0039-9140\(01\)00323-X](https://doi.org/10.1016/S0039-9140(01)00323-X).
35. V. Veronico, P. Favia, F. Fracassi, R. Gristina, and E. Sardella, "Validation of Colorimetric Assays for Hydrogen Peroxide, Nitrate and Nitrite Ions in Complex Plasma-Treated Water Solutions," *Plasma Processes and Polymers* 18, no. 10 (2021): 2100062, <https://doi.org/10.1002/ppap.202100062>.
36. F. J. Richards, "A Flexible Growth Function for Empirical Use," *Journal of Experimental Botany* 10, no. 2 (1959): 290–301, <https://doi.org/10.1093/jxb/10.2.290>.
37. Y. Hara, "Calculation of Population Parameters Using Richards Function and Application of Indices of Growth and Seed Vigor to Rice Plants," *Plant Production Science* 2, no. 2 (1999): 129–135, <https://doi.org/10.1626/ppp.2.129>.
38. K. Hartmut, "Chlorophylls and Carotenoids: Pigments of Photosynthetic Biomembranes," *Methods in Enzymology* 148 (1987): 350–382.
39. C. Bailly, "Active Oxygen Species and Antioxidants in Seed Biology," *Seed Science Research* 14, no. 2 (2004): 93–107, <https://doi.org/10.1079/ssr2004159>.
40. K. Kučerová, M. Henselová, L. Slováková, and K. Hensel, "Effects of Plasma Activated Water on Wheat: Germination, Growth Parameters, Photosynthetic Pigments, Soluble Protein Content, and Antioxidant Enzymes Activity," *Plasma Processes and Polymers* 16, no. 3 (2019): 1800131, <https://doi.org/10.1002/PPAP.201800131>.
41. V. Stoleru, R. Burlica, G. Mihalache, et al., "Plant Growth Promotion Effect of Plasma Activated Water on *Lactuca sativa* L. Cultivated in Two Different Volumes of Substrate," *Scientific Reports* 10, no. 1 (2020): 20920, <https://doi.org/10.1038/s41598-020-77355-w>.
42. K. Kučerová, M. Henselová, L. Slováková, M. Bačovčinová, and K. Hensel, "Effect of Plasma Activated Water, Hydrogen Peroxide, and Nitrates on Lettuce Growth and Its Physiological Parameters," *Applied Sciences* 11, no. 5 (February 2021): 1–14, <https://doi.org/10.3390/app11051985>.
43. K. Kučerová, Z. Machala, and K. Hensel, "Transient Spark Discharge Generated in Various N₂/O₂ Gas Mixtures: Reactive Species in the Gas and Water and Their Antibacterial Effects," *Plasma Chemistry and Plasma Processing* 40, no. 3 (2020): 749–773, <https://doi.org/10.1007/s11090-020-10082-2>.
44. G. B. N. Yemeli, M. Janda, and Z. Machala, "Non-Thermal Plasma as a Priming Tool to Improve the Yield of Pea in Outdoor Conditions," *Plasma Chemistry and Plasma Processing* 42, no. 5 (2022): 1143–1168, <https://doi.org/10.1007/s11090-022-10264-0>.
45. D. Kostoláni, G. B. Ndiiffo Yemeli, R. Švubová, S. Kyzek, and Z. Machala, "Physiological Responses of Young Pea and Barley Seedlings to Plasma-Activated Water," *Plants* 10, no. 8 (2021): 1750, <https://doi.org/10.3390/plants10081750>.
46. P. Silapasert, C. Yatonchai, and S. Sarapirom, "Investigation of Plasma Activated Water in the Growth of Green Microalgae (*Chlorella* spp.)," *Journal of Physics: Conference Series* 2431, no. 1 (2023): 012037, <https://doi.org/10.1088/1742-6596/2431/1/012037>.
47. H. H. Sinaga, H. Al Falaq, N. Purwasih, and D. Permata, "Water Treatment Using Plasma Generated by High Voltage Tesla Transformer to Eliminate *Escherichia coli* Bacteria," in *Proceedings ICCTEIE 2021 2021 International Conference on Converging Technology in Electrical and Information Engineering, Converging Technology for Sustainable Society* (2021): 10–13, IEEE, <https://doi.org/10.1109/ICCTEIE54047.2021.9650631>.
48. P. Jamróz, K. Gręda, P. Pohl, and W. Żyrmicki, "Atmospheric Pressure Glow Discharges Generated in Contact With Flowing Liquid Cathode: Production of Active Species and Application in Wastewater Purification Processes," *Plasma Chemistry and Plasma Processing* 34, no. 1 (2014): 25–37, <https://doi.org/10.1007/s11090-013-9503-3>.
49. D. Dobrin, M. Magureanu, N. B. Mandache, and M. D. Ionita, "The Effect of Non-Thermal Plasma Treatment on Wheat Germination and Early Growth," *Innovative Food Science & Emerging Technologies* 29 (2015): 255–260, <https://doi.org/10.1016/j.ifset.2015.02.006>.
50. I. K. Naumova, A. I. Maksimov, and A. V. Khlyustova, "Stimulation of the Germinability of Seeds and Germ Growth Under Treatment With Plasma-Activated Water," *Surface Engineering and Applied Electrochemistry* 47, no. 3 (2011): 263–265, <https://doi.org/10.3103/S1068375511030136>.
51. M. Ashraf, "Biotechnological Approach of Improving Plant Salt Tolerance Using Antioxidants as Markers," *Biotechnology Advances* 27, no. 1 (2009): 84–93, <https://doi.org/10.1016/j.biotechadv.2008.09.003>.
52. L. A. Del Río, "ROS and RNS in Plant Physiology: An Overview," *Journal of Experimental Botany* 66, no. 10 (2015): 2827–2837, <https://doi.org/10.1093/jxb/erv099>.
53. D. P. Park, K. Davis, S. Gilani, et al., "Reactive Nitrogen Species Produced in Water by Non-Equilibrium Plasma Increase Plant Growth Rate and Nutritional Yield," supplement, *Current Applied Physics* 13, no. SUPPL.1 (2013): 1–11, <https://doi.org/10.1016/j.cap.2012.12.019>.
54. T. P. Kasih, R. Purwondho, D. Danil, R. Radjagukguk, and A. Bagaskara, "Germination Enhancement of Green Bell Pepper (*Capiscum annuum* L) by Using Non Thermal Argon Plasma," in *IOP Conference Series: Earth and Environmental Science* 426, no. 1 (IOP, 2020): 012131, <https://doi.org/10.1088/1755-1315/426/1/012131>.
55. M. Măgureanu, R. Sîrbu, D. Dobrin, and M. Gidea, "Stimulation of the Germination and Early Growth of Tomato Seeds by Non-Thermal Plasma," *Plasma Chemistry and Plasma Processing* 38, no. 5 (2018): 989–1001, <https://doi.org/10.1007/s11090-018-9916-0>.
56. M. C. Pérez-Pizá, E. Cejas, C. Zilli, et al., "Enhancement of Soybean Nodulation by Seed Treatment With Non-Thermal Plasmas," *Scientific Reports* 10, no. 1 (2020): 4917, <https://doi.org/10.1038/s41598-020-61913-3>.
57. M. Bafail, A. Jemmat, Y. Martinez, et al., "Effects of Low Temperature Plasmas and Plasma Activated Waters on *Arabidopsis thaliana* Germination and Growth," *PLoS One* 13, no. 4 (2018): 1–16, <https://doi.org/10.1371/journal.pone.0195512>.
58. D. Li, J. Limwachiranon, L. Li, et al., "Hydrogen Peroxide Accelerated the Lignification Process of Bamboo Shoots by Activating the Phenylpropanoid Pathway and Programmed Cell Death in Postharvest Storage," *Postharvest Biology and Technology* 153 (2019): 79–86, <https://doi.org/10.1016/j.postharvbio.2019.03.012>.
59. Y. Wang, M. Chantreau, R. Sibout, and S. Hawkins, "Plant Cell Wall Lignification and Monolignol Metabolism," *Frontiers of Plant Science* 4, no. JUL (2013): 220, <https://doi.org/10.3389/fpls.2013.00220>.

60. V. Stoleru, C. Stratulat, G. Teliban, et al., "Morphological, Physiological and Productive Indicators of Lettuce under Non-Thermal Plasma," in *EPE 2018 - Proceedings 2018 10th International Conference Exposition on Electrical and Power Engineering* (IEEE, 2018), 937–942, <https://doi.org/10.1109/ICEPE.2018.8559894>.
61. F. H. Ruiz-Espinoza, B. Murillo-Amador, J. L. García-Hernández, et al., "Field Evaluation of the Relationship Between Chlorophyll Content in Basil Leaves and a Portable Chlorophyll Meter (SPAD-502) Readings," *Journal of Plant Nutrition* 33, no. 3 (2010): 423–438, <https://doi.org/10.1080/01904160903470463>.
62. M. Havaux, "Carotenoid Oxidation Products as Stress Signals in Plants," *Plant Journal* 79, no. 4 (2014): 597–606, <https://doi.org/10.1111/tip.12386>.
63. P. Sharma, A. B. Jha, R. S. Dubey, and M. Pessarakli, "Reactive Oxygen Species, Oxidative Damage, and Antioxidative Defense Mechanism in Plants Under Stressful Conditions," *Journal of Botany* 2012 (2012): 1–26, <https://doi.org/10.1155/2012/217037>.